

# Trailing Ballute Aerocapture: Concept and Feasibility Assessment

Jake Lewis<sup>†</sup>, Kevin L. Miller<sup>‡</sup>, Bill Trochman<sup>†</sup>  
*Ball Aerospace & Technologies Corp., Boulder, CO*

Jim Stein\*  
*ILC Dover, Inc., Frederica, DE*

Daniel T. Lyons \*  
*Jet Propulsion Laboratory, California Institute of Technology, Pasadena, CA*

Richard G. Wilmoth\*  
*NASA Langley Research Center, Hampton, VA*

Trailing Ballute Aerocapture offers the potential to obtain orbit insertion around a planetary body at a fraction of the mass of traditional methods. This allows for lower costs for launch, faster flight times and additional mass available for science payloads. The technique involves an inflated ballute (balloon-parachute) that provides aerodynamic drag area for use in the atmosphere of a planetary body to provide for orbit insertion in a relatively benign heating environment. To account for atmospheric, navigation and other uncertainties, the ballute is oversized and detached once the desired velocity change ( $\Delta V$ ) has been achieved. Analysis and trades have been performed for the purpose of assessing the feasibility of the technique including aerophysics, material assessments, inflation system and deployment sequence and dynamics, configuration trades, ballute separation and trajectory analysis. Outlined is the technology development required for advancing the technique to a level that would allow it to be viable for use in space exploration missions.

*keywords:* aerocapture, inflatable, thin-film structures, rarefied flow, direct simulation monte carlo (DSMC)

<sup>†</sup> Member AIAA

\* Co-Investigator, Member AIAA

<sup>‡</sup> Principal Investigator, Member AIAA

---

## Nomenclature

$Kn$	Knudsen number
$M$	Mach number
$p$	pressure
$q$	heating rate

## Introduction

The application of inflatable film systems for aeroassist maneuvers has been employed in system designs for over 20 <TBR> years<sup>1</sup>. A team consisting of Ball Aerospace and Technologies, Corp., ILC Dover, Inc., Jet Propulsion Lab, and Langley Research Center has been engaged over the past 2 years developing critical technologies and analyses for the use of balloon-parachutes (bal-

lutes) for capture in a planetary orbit using the atmosphere to generate aerodynamic drag, thus slowing the system to capture into a desired orbit. Using specific impulse as a means of illustrating performance relative to other technologies, such as chemical propulsion, ballutes provide up to 1200 s impulse, yet retain scalability over a large range of spacecraft size without significantly constraining the spacecraft operations or configuration. For an orbital mass of 1000 kg and a delta V of 1 km/s, this results in an increase in payload mass (or a reduction of launch mass) of over 350 kg.

This paper addresses critical issues for implementation of the technology, mission design constraints, configuration concepts and overall performance characteristics, including results of aerothermal and aerostability analyses, guidance algorithm design and performance, and overall system characteristics. The effort to date has focused on capture at Mars and Titan. Future efforts

---

Copyright © 2003 by Ball Aerospace & Technologies Corp. Published by the American Institute of Aeronautics and Astronautics, Inc. with permission.

will include detailed analysis of Neptune mission options.

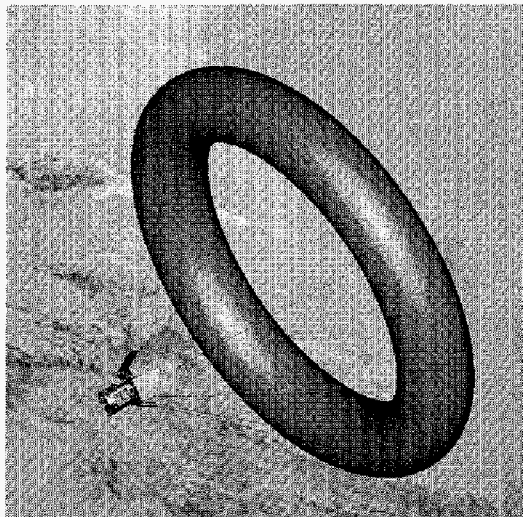


**Fig. 1. Ballute aerocapture provides orbit insertion with small influence on spacecraft design and a mass fraction of less than 25 percent, saving hundreds of kilograms as contrasted with traditional techniques.**

### Mission Concept

Ballute technology can be applied with many configuration options and design approaches, but the overall mission concept investigated in this paper begins with the material limitations of the ballute system, and establishes mission designs that are compatible with these limitations. More specifically, the design logic illustrated in Figure 1 is employed to define primary characteristics and limitations of the flight system.

The flight system is launched with the inflatable system stowed, and remains in this configuration throughout most of cruise. A candidate aerocapture sequence is illustrated in Table 2 <insert D. Lyons table>. As shown, a day or two prior to the projected atmospheric entry interface, the ballute system is deployed and inflated, allowing ample time for damping of deployment dynamics and verification of the entry configuration. A final trajectory correction maneuver may be conducted shortly before entry to minimize the delivery error term. Although attitude error and atmospheric instabilities perturb the flight system, the restoring moment with the trailing ballute is so large that static aerodynamic stability is not a major issue. The periapsis is targeted to keep peak heating rates within the ballute material limits for the drag modulated atmospheric pass. The ballute drag area is sized to provide sufficient delta velocity to capture in the desired orbit. As discussed in Guidance and Separation Performance, the on-board computer and accelerometers are used to calculate a point for separation of the ballute system based on the projected delta V of the towing spacecraft at atmospheric exit. After com-

manding a pyro-initiated separation, the towing spacecraft completes a ballistic trajectory to the atmospheric exit point. A propulsive burn is conducted at apoapsis to raise periapsis out of the atmosphere.

Three of the key challenges to be faced in the development of an aerocapture mission are: (1) navigation, trajectory management, and atmospheric characteristics, (2) aerostability of the spacecraft during the aeropass, including deployments and aeroelastic response of the system to hypersonic environments, and (3) development of spacecraft systems capable of sustaining the very high heating rates and aerodynamic forces of aerocapture, without sustaining excessive impact on the overall mission.

The following figures show a comparison between two representative aerocapture trajectories: one for Mars and one for Titan. The 5.5 km/sec entry speed for the Mars trajectory is representative for a direct Earth to Mars type 1 trajectory launched in 2005. The 6.5 km/sec entry speed for the Titan trajectory is representative of a Solar Electric Propulsion trajectory with a single Venus flyby and a flight time of about 7 years. Table 2 specifies the key parameters for each trajectory.

Table 2: Key Parameters

Parameter	Mars	Titan
Entry Mass	400 kg	500 kg
Ballute Mass	25 kg	41 kg
Area with Ballute	300 m <sup>2</sup>	751 m <sup>2</sup>
Area without Ballute	2 m <sup>2</sup>	x m <sup>2</sup>
Entry C <sub>D</sub>	1.7	1.7
S/C C <sub>D</sub>	1.8	x
Entry Speed	5.5 km/sec	6.5 km/sec
Max. Allowable Qdot	3.0 W/cm <sup>2</sup>	3.0 W/cm <sup>2</sup>
Entry Flight Path Angle	-22°	-39°
Entry Altitude	200 km	1000 km
Atmo Scale Height	7.6 km	41 km
Pass duration		
Ballistic Ratio		

The periapsis altitude of the hyperbolic approach trajectories was targeted low enough to accommodate reasonable uncertainties in entry conditions due to Nav errors as well as reasonable uncertainties in the atmospheric density. Thus, a high periapsis altitude (equivalent to a shallow Flight Path Angle at entry) and a low density atmosphere would require drag from the ballute

for the entire pass through the atmosphere. For the nominal entry conditions and atmospheres used for these representative trajectories, sufficient delta-V is achieved before the spacecraft reaches periapsis, so the ballute must be released to minimize the drag during the remainder of the flight through the atmosphere.

Figure 2.0 shows a typical sequence of events during the ballute aerocapture phase. The spacecraft approaches the planet or moon on a hyperbolic approach trajectory (1) that has been carefully targeted to enter the atmosphere (2) at the desired speed and flight path angle. The large drag from the ballute system causes the spacecraft to experience a maximum deceleration of several g's (3) shortly after entry. When the spacecraft has been slowed sufficiently the ballute is released (4) and the spacecraft proceeds through the remainder of the atmospheric segment (5-7) with minimal drag. If too much energy is removed from the orbit before leaving the atmosphere, a drag makeup maneuver (6) might be required to raise apoapsis out of the atmosphere. A maneuver at the first apoapsis (8) is essential for raising periapsis out of the atmosphere. If the on-board orbit determination is sufficiently accurate, the periapsis raise maneuver can be targeted very close to the desired final altitude so that a single, final maneuver can be made to circularize the orbit (9). The alternative is to command several "clean-up" maneuvers from the ground after tracking the spacecraft after the automated maneuvers have put the spacecraft close to its final, science orbit.

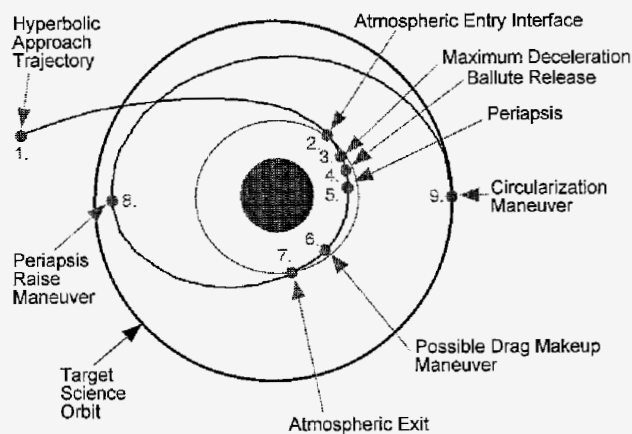


Figure 2.0 Sequence of Events for a Representative Ballute Aerocapture

Figure 3 shows the time history of the altitude during the atmospheric flight segment of the representative trajectories. The initial state is 100-200 sec before entry, which is defined at a particular altitude for each body. The entry and release times are noted by dashed lines on the plots, where Titan entry (and Release) occurs before Mars entry (and Release) only because the time from

entry for the initial states were arbitrarily specified. The ballutes are released before periapsis is reached for both examples because the nominal trajectory is targeted low enough to accommodate uncertainties. Note that the Titan atmosphere is much thicker than for Mars, since entry is at 1000 km altitude for Titan and at 200 km for Mars.

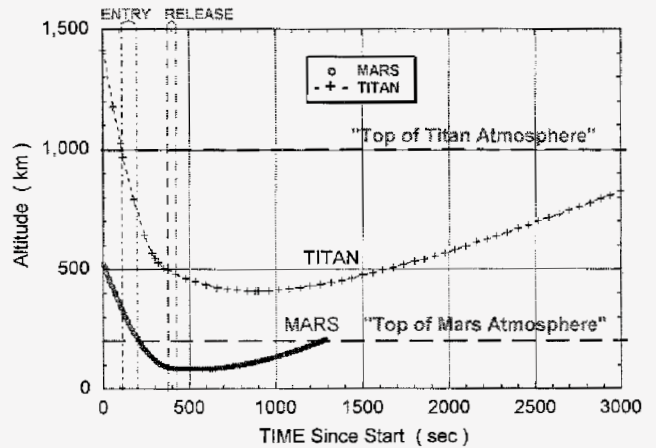


Figure 3: Altitude versus Time for Representative Ballute Aerocapture at Mars & Titan

Figure 4 shows the velocity history during the atmospheric flight segment. Trajectories for Titan are expected to have a higher entry speed and Delta V than for Mars. The velocity decreases rapidly early in the trajectory when the velocity is high and the density is increasing rapidly. For both of these cases, ballute release may be at a relatively high altitude well before periapsis, so there is enough towing spacecraft drag during the remainder of the trajectory to have a noticeable effect on the velocity. This effect must be estimated by the on-board separation algorithm in order to release the ballute at the correct time. (These trajectories were the result of a computer search for the right time to separate, so both hit their respective apoapsis targets exactly.) In the real world there is some chance that the ballute will be released a little too soon, in which case drag will not provide enough velocity change and propellant will be used to lower the apoapsis altitude later in the mission. There is also a chance that the ballute will be released late, in which case drag will extract too much energy from the orbit, and propellant will be used to raise the apoapsis later in the orbit. If release is significantly later than the perfect release time (i.e., ~3-5 sec), propellant will be needed during the pass to raise apoapsis. This burn is pre-programmed and selected based on on-board sensing.

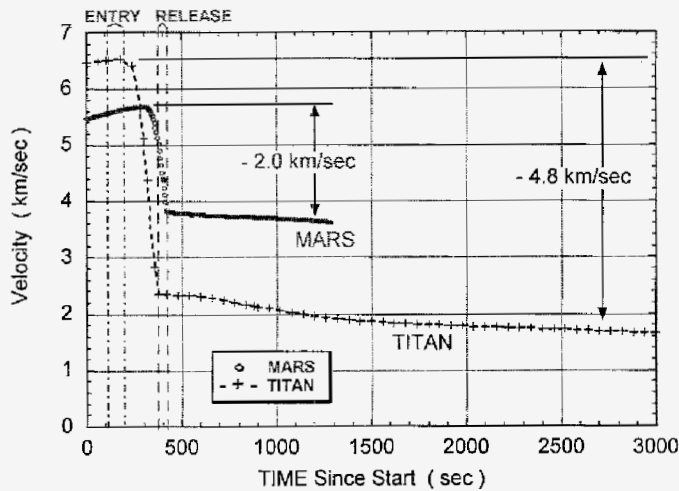


Figure 4: Velocity versus Time for Representative Ballute Aerocapture at Mars & Titan

A basic assumption for this study was that the ballute would be made out of existing materials, such as Kapton. Kapton has a rated temperature of about 500°C, which corresponds with a heating rate of about 3 W/cm<sup>2</sup>. The size of the ballute is selected based on this. Figure 5 shows maximum Qdot prior to ballute release. In these examples, there is a secondary peak near perapsis, where the density is highest. If the entry flight path angle is decreased (undershoot, i.e. the approach hyperbola is targeted to a lower altitude), then the ballute will be released earlier than for these reference trajectories, and the secondary peak will be larger. If the entry path is steep enough, then the secondary peak can be larger than the primary peak. Steeper entries have a much more noticeable effect on the secondary peak than they do on the primary peak, since the ballute can still be attached. Although the ballute does not have to survive the secondary peak, because it has already been released, the spacecraft does have to survive both peaks. Higher peaks require more thermal protection of the spacecraft. An atmospheric density that is significantly higher than nominal has the same effect on the shape and magnitudes of the peaks as a steeper entry. Conversely, a shallower entry, or a thinner than expected atmosphere have the opposite effect in that both the Qdot peaks before and after ballute release are reduced. Better knowledge of the atmosphere and better navigation both enable the approach trajectory to be targeted higher in the atmosphere, where both Qdot and uncertainties due to separation errors are minimized.

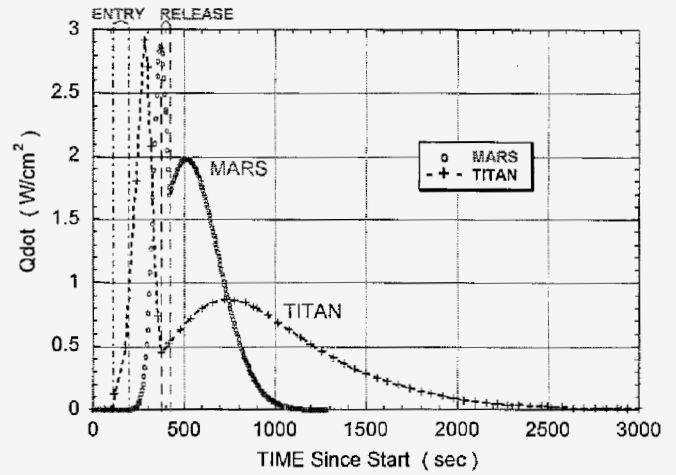


Figure 5: "Qdot" versus Time for Representative Ballute Aerocapture at Mars & Titan

Figure 6 shows the Dynamic Pressure (defined as  $0.5 * \text{Density} * \text{Velocity}^2$ ). While the ballute is attached, the dynamic pressure is useful for computing how much inflation pressure, aeroelastic effects and tether loads..

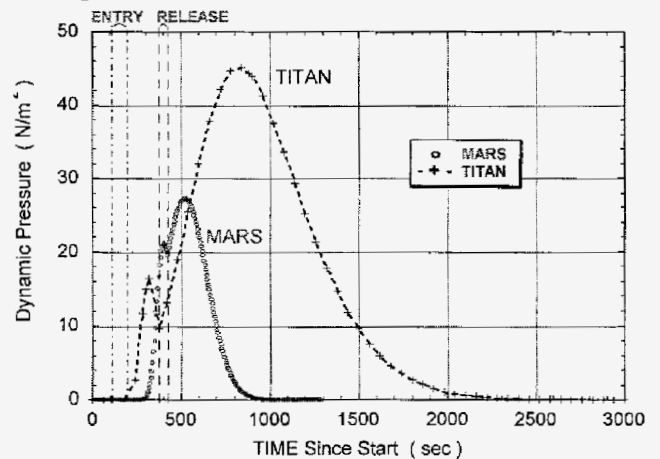


Figure 6: Dynamic Pressure versus Time for Representative Ballute Aerocapture at Mars & Titan

When the system enters the atmosphere, the large drag area results in a rapid deceleration that can reach several g's before the spacecraft has decelerated enough, as shown in Figure 7. The rate of increase and the magnitude of the peak always occur before separation, so they are useful measurements that can improve the performance of the separation algorithm. Once the ballute is released, the deceleration drops dramatically because the drag area is typically reduced by up to a factor of 150, or the ratio of the ballistic number of the towing spacecraft and the towing spacecraft plus ballute. The deceleration usually remains very low after ballute re-

lease even though the maximum dynamic pressure is largest near periapsis.

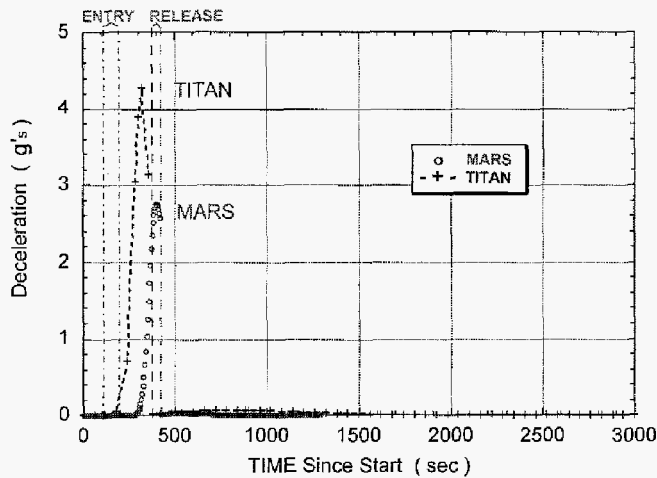


Figure 7.7: Deceleration versus Time for Representative Ballute Aerocapture at Mars & Titan

Figure 8 shows the history of the atmospheric density during the atmospheric flight segment. While the ballute is attached, the densities are very comparable between Mars and Titan. After ballute release, the density at periapsis of the Titan trajectory is significantly higher than for the Mars trajectory. Even though the density is larger for this Titan trajectory, the secondary peak for  $Q_{dot}$  is less than for the Mars trajectory, because the velocity is lower.

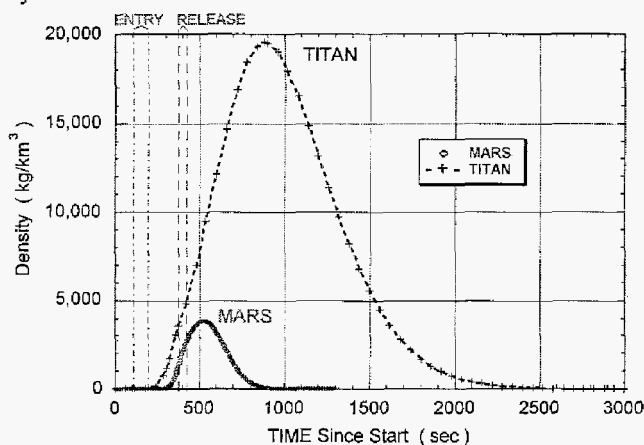


Figure 8: Density versus Time for Representative Ballute Aerocapture at Mars & Titan

Figure 9 shows the log of the density plotted versus altitude for these two reference trajectories. The significantly steeper slope for the Mars example represents the much smaller scale height for the Mars atmosphere (7.6 km) than that for Titan (41 km).

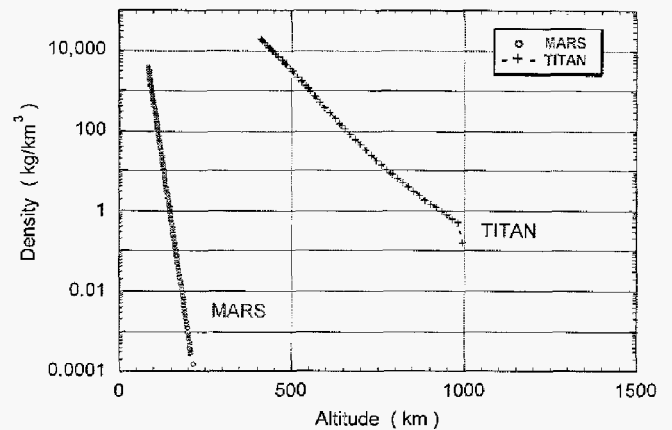
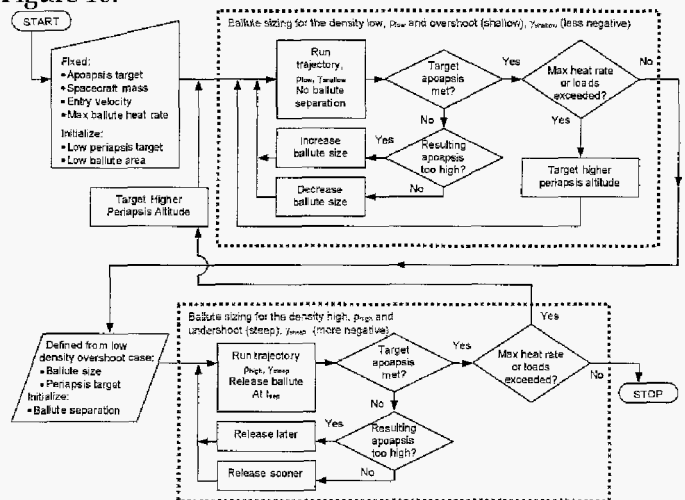


Figure 9: Density versus Altitude for Representative Ballute Aerocapture at Mars & Titan

### Configuration Concept

A variety of configuration concepts employing ballute technology can be applied for planetary aerocapture missions, but this paper is focused on the use of trailing toroidal ballutes. As presented by Masciarellia and Westhelle, ballistic ratio is a key design parameter. In order to minimize the size and mass of the ballute assembly, the towing spacecraft ballistic number is maximized. General logic for sizing of a ballute system is illustrated in Figure 10.



The frontal area of the ballute is determined by the delta V requirement of the mission. For a toroidal ballute the remainder of the geometry is then dependent on the aspect ratio (major diameter/minor diameter). For a given frontal area the surface area of the ballute remains constant. Thus the weight of the thin film comprising the ballute is independent of the aspect ratio. However, the gas volume decreases with increasing aspect ratio, so the more the ballute resembles a bicycle tire instead of a

truck tire, the lighter the ballute will be. This mass savings is somewhat offset by the additional weight of longer tethers used to support a large aspect ratio ballute. For a 750 m<sup>2</sup> frontal area ballute with an aspect ratio of 5:1 the inflation gas mass is 1/3 of the thin film mass of the ballute.

The toroidal ballutes provide many advantages for aero capture, such as spacecraft wake swallowing to minimize heating impacts. However, other shapes have also been investigated. For example, a double torus, which is two toroids with a flat span of material between them, is also a possible candidate. This geometry does not tend to produce significant film mass savings but can substantially reduce the required mass of the inflation gas. The double torus is a more complicated geometry and would also probably require more mass for seaming.

The tether angle is sized by determining the distance the ballute needs to trail behind the spacecraft for the spacecraft wake to be swallowed by the hole in the torus. This is also a function of ballute aspect ratio. Lower tether angles result in lower tether and ballute loads but are also longer which increases tether mass.

Tethers can be grouped into two primary categories, strings and columns. String tethers provide stiffness in tension only whereas columns provide both tension and compression stiffness. Column tethers are desirable because they provide a stable and verifiable configuration before entering the atmosphere. String tethers introduce the risk of recontact between the ballute and spacecraft and uncontrolled attitude upon atmospheric entry. Deployment of the ballute during the drag pass, like a parachute deployment, is possible but riskier. With drag deployment it might not be necessary to have column tethers because string tethers would always be in tension. A mix of string and column tethers may be the best option. String tethers provide a greater range of material possibilities and can probably be more efficient in tension than column tethers which are likely to be inflated tubes of the same material as the ballute.

### **Risk and Critical Issues**

Ballutes offer significant, and in some cases, enabling capability for missions to 8 bodies, as indicated in Table 1. However, there are a number of critical technology issues that must be retired before the apparent performance advantages may be realized.

<Use table of top technical risks >

### **Analysis Tool Discussion**

The aerothermodynamic design objectives for an inflatable aerocapture system are to maximize the drag

while minimizing the aerodynamic heating so as to minimize the non-payload weight. Approximate design tools are used to initially size the aerocapture device, but the complexity of the flow around ballute geometries requires that these designs be verified and design margins be established through detailed aerothermodynamic analyses. Furthermore, an initial review of the trade space for Neptune and Titan aerocapture suggests that peak heating could occur over a wide range of flow regimes ranging from hypersonic continuum to transitional rarefied flow. Therefore, analysis techniques are required that can fully address the issues associated with each of these regimes.

In the continuum regime, the LAURA (Langley Aerothermodynamic Upwind Relaxation Algorithm) code [Gnoffo 1990] provides the capability to model hypersonic, high-temperature real-gas flows based on the Navier-Stokes equations. LAURA has been previously applied to computations of toroidal geometries for nominal aerocapture conditions for several different planetary atmospheres including Neptune and Titan [Gnoffo 2001]. The thermochemical models developed for these earlier studies include finite-rate chemistry and are used in the present work.

At lower densities, flow around the spacecraft and ballute transitions to rarefied flow, and aerothermodynamic simulations require the Direct Simulation Monte Carlo (DSMC) technique developed by Bird [Bird, 1994]. DSMC simulates gas flows by modeling the motion and collisions of millions of representative molecules based on the kinetic theory of gases. For this study, the DAC code (DSMC Analysis Code) of LeBeau [LeBeau 2001] is used. DAC treats complex three-dimensional geometries as well as simple axisymmetric shapes while simulating the discrete molecular behavior of the flow with multiple species including chemistry. DAC chemistry models were developed based on the same reaction sets and rates used in the LAURA continuum calculations.

The Navier-Stokes and DSMC simulations are supplemented with rapid-design, engineering methods based on free-molecular and Newtonian models, continuum-to-rarefied bridging relations, and stagnation heating correlations. The detailed results obtained from the Navier-Stokes and DSMC simulations allow an assessment of the error margins that should be applied to the engineering methods as well as providing more detailed predictions of force and heating distributions.

### **Performance Analysis Results**

#### **Aeroanalysis Results**

Navier-Stokes (LAURA) and DSMC (DAC) simulations have been performed for a 750 m<sup>2</sup> ballute at several points along a typical Titan aerocapture trajectory to provide aerodynamic drag and heating environments.

The LAURA simulations were performed with no-slip, radiative equilibrium, and fully-catalytic wall boundary conditions. Thermal nonequilibrium was treated with a two-temperature gas model. The DSMC simulations were performed using fully diffuse wall boundaries with complete thermal accommodation and fully catalytic recombination of atomic species. LAURA and DAC were run for several of the same trajectory conditions to provide overlap between continuum and rarefied predictions.

A sample DSMC flowfield prediction is shown in Fig. 11. (Since the flow is axisymmetric, only the region from the axis to the outer computational boundary is shown.) The bow shock created by the toroid focuses to a triple point above the axis formed at the intersection with a normal shock (Mach disk) and reflected shock. For trajectory conditions where both LAURA and DAC were run, similar flow structures were obtained, and the variation in the size and location of the Mach disk over the trajectory was similar for the two methods.

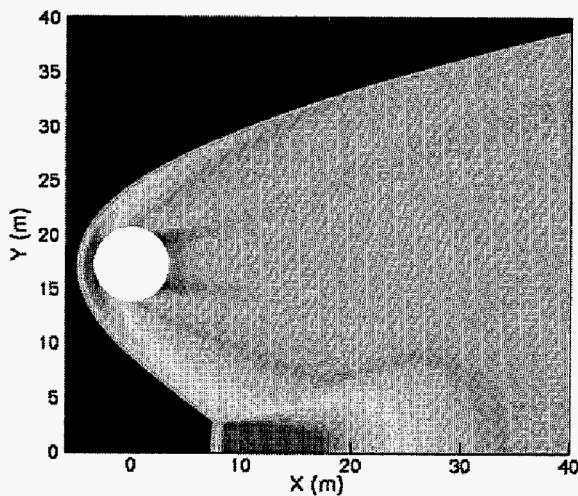


Figure 11 - Pressure Contours for DSMC Prediction Near Peak Heating Condition.  $V_\infty=5.52$  km/s,  $\rho_\infty=9.04 \times 10^{-7}$  kg/m<sup>3</sup>,  $T=168$  K.

Aerodynamic drag predictions are shown as a function of Knudsen number in Fig. 12 where the Knudsen number is based on the maximum ballute diameter. The predictions are compared to a traditional bridging relation based on a sine-squared variation in drag between the continuum and free-molecular limits. The bridging relation was developed prior to the computational simulations and used to predict ballute drag in the initial trajectory determination. The bridging relation could likely be improved by basing the Knudsen number on the minor diameter rather than the maximum diameter of the toroid. However, the LAURA and DAC predictions show that the original bridging relation gives a conserva-

tive (lower) prediction of the drag effectiveness of the ballute.

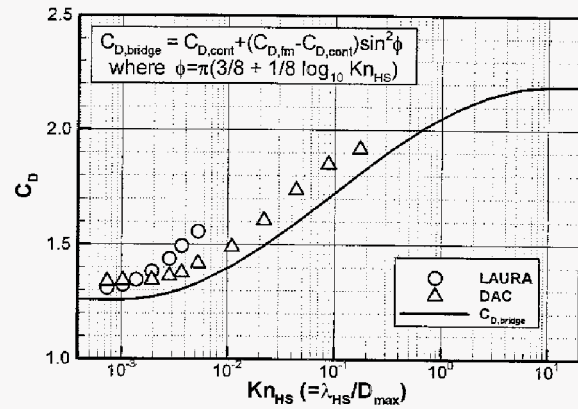


Figure 12 - Ballute Drag Coefficient - Comparison of CFD/DSMC Predictions to Bridging Relation

The stagnation heat transfer on the ballute is shown as a function of density along the trajectory in Fig. 13. The peak heating condition occurs at a condition where rarefaction effects become increasingly important. The predictions correlate well with  $\rho_\infty^{0.5} V_\infty^3$  as expected for these hypersonic flow conditions, and this correlation is extended to very low densities using a bridging relation similar to that used for drag. LAURA predicts higher heating than DAC at densities less than  $10^{-6}$  kg/m<sup>3</sup> in part due to lack of slip boundary conditions in the LAURA calculations. However, assessment of these differences should be made with caution since there are differences in the details of the thermal and chemical modeling between the two methods whose effects have not been fully investigated.

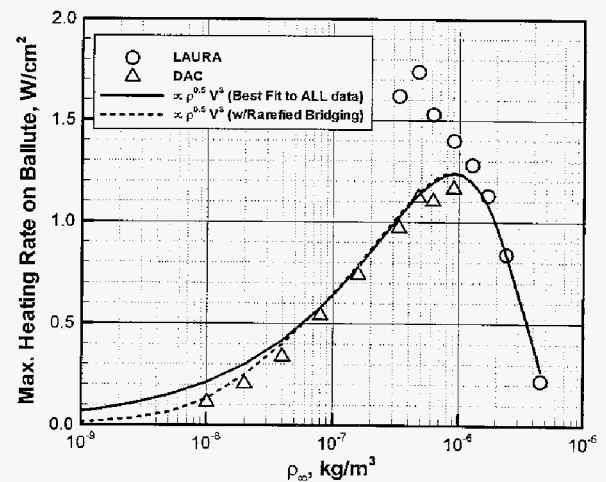


Figure 13 - Correlation of Stagnation Heating Rate  
Aeroheating/Thermal Response

Analyses have been developed to ensure that the ballute system is maintained within limits of the inflatable system. A temperature response curve for maximum aerocapture heating at Titan is illustrated in Figure 14. Although the majority of the system is comprised of lightweight films 0.5 mil thick and less, in some localized areas, due to reduced nose radii and consequently, increased local heating, , somewhat heavier materials with higher temperature limits will be employed.

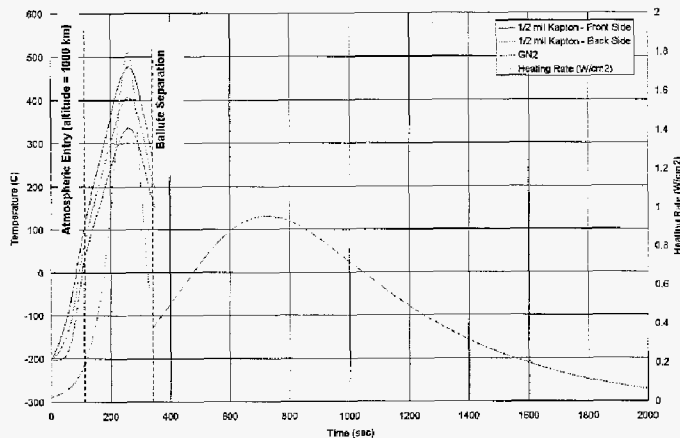


Figure 14 – The ballute trajectory design has been shaped by material performance limits of 500°C.

### Manufacturing and Material Performance Considerations

The driving constraint for ballute aerocapture is the ballute material property limits. Aero-thermal analyses have been used to create a configuration that meets the performance requirements for the ballute and achieves a thermal environment that is near the limits of state-of-the-art materials. For several of the materials discussed below, the thermal environment is beyond their published glass-transition temperatures ( $T_g$ ). However, due to the transient nature of the aerocapture event, these materials remain viable candidates because they support the loading conditions during the event even as they degrade. With these candidates, manufacturing, especially seam development, provides the greatest materials challenge in regards to the thermal environment.

To begin, a broad range of potential materials

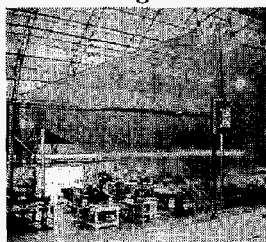


Figure XX. ILC Dover ISIS Sunshield demonstrates the maturity of seaming, fabrication, and deployment of large, thin-film Kapton structures

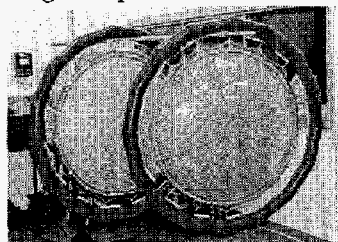


Figure XX. ILC Dover parabolic antenna reflector dish demonstrates the capability of 3-dimensional forming of Kapton film structures

were identified. For the inflatable

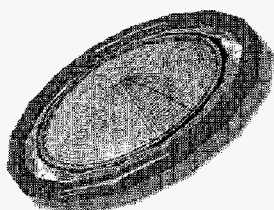


Figure XX ILC Dover parabolic antenna reflector

toroid and tethers,

candidates include thin films, “rigidizable” composites, elastomer-coated structural fabrics, and ceramic fabrics (i.e. Nextel, Fiberfrax). Operating temperature limits for these materials range from 125°C to 1250°C. The two leading candidate materials identified were thin films: Kapton and Polyboxoxazole (PBO). Both Kapton and PBO offer relatively high temperature capabilities—around 500 °C. PBO is reported to perform at even higher temperatures, however further material study is required. PBO film is currently produced at the research and development level, which involves a blown film process whereby a 7-in. diameter tubular extrusion is slit to obtain a 22-in. flat width. PBO also remains flexible at cryogenic temperatures, unlike other high-temperature film candidates. In contrast, Kapton film is cast and is very mature from a manufacturing standpoint. It is relatively inexpensive, available off-the-shelf, has flight heritage (TRL 9), and has similar performance characteristics as PBO.

For tensile tethers, high strength materials such as PBO and Twaron are available; more advanced materials such as MSI’s M5, currently at a low TRL, will be monitored as it is developed. These materials are typically capable of operating at temperatures up to 650°C for limited periods of time. To increase tether performance at temperature, a ceramic jacketing is a viable option, if necessary, to protect the tether during aerocapture.

To identify viable materials for a ballute, a variety of mechanical tests of candidate materials are currently being performed using a Dynamic Mechanical Analyzer (DMA). This equipment provides a means to compare Modulus (both stored and loss), creep performance (both isothermal and ramping temperature), and tensile performance. The DMA allows testing at temperatures of up to 650°C and in a controlled atmosphere. For the current effort, a nitrogen purge is being used because it is representative of aerocapture targets and it is non-oxidizing. Additional optical testing will also be performed to determine emissivity properties of the candidates. This trade will identify those films that are more likely to radiate thermal energy away from the ballute and reduce surface temperatures.

The material trade extends beyond material maturity and temperature performance. Seaming these materials will require development for this type of application. Temperature survivability of the ballute assembly depends on the capability of seam construction more so than that of the base material. Several techniques currently exist and have been employed on thin film structures. For example, pressure sensitive adhesive (PSA) tapes are commonly employed due to their ease of use with thin films. Unfortunately, PSA’s do not operate at high environmental temperatures without the aid of thermal protection.

To maintain low-mass seams, polyimide adhesives and high temperature silicone adhesives are being investigated for seam construction. Polyimide adhesives are of the same polymer family as Kapton, only in liquid form. These can be difficult to work with on a large scale because it requires a very high temperature and moderate pressure to create the bond. In some cases, the temperature required is very near the base material limits. However, the resulting bond is at (or near) the full strength of the base material because it creates a bond at a molecular level. Silicone adhesives are available in many forms from room temperature vulcanized (RTV) to platinum/heat cured. This system will rely on a mechanical bond to the film to achieve its strength. However, many films are not overly receptive to a silicone bond so special candidates must be selected. For this assessment, coated films have been identified that are high temperature capable. These include vapor-deposited aluminum (VDA) films, copper coated films, and germanium coated films. In addition to bond capability, it is expected that these metalized films will improve emissivity and ESD protection.

Another manufacturing issue that must be considered is the material patterning approach. Since materials are not available in a width of the scale of the ballute, it must be broken into smaller seamed sections. The typical approach for an inflatable torus is to pattern it as segments. The smaller (and more numerous) the segments, the less faceted and more ideal shaped of the torus will be achieved. However, the greater the number of segments, the more seams exist, increasing manufacturing time and cost as well as mass. To alleviate this problem, thermal forming of films is being assessed. Kapton films have been successfully 3-dimensionally formed to create a more conformal shape for inflatables such as a parabolic antenna reflector dish. This forming process involves moderate effort to develop molds that produce high quality formed parts. Ultimately, the patterned shape will be traded against the predicted aero/thermal performance to determine the design and manufacturing approach.

### Guidance and Separation Performance

A successful ballute aerocapture, which leaves the towing spacecraft in the desired orbit, requires release of the ballute after sufficient energy loss is achieved. The timing of the ballute separation must be robust enough to handle atmospheric density uncertainties, entry trajectory delivery and knowledge errors and spacecraft and ballute ballistic coefficient uncertainties. Ballute separation timing is performed on-board by comparing the desired and estimated orbital energy. Orbital energy is estimated by propagating the trajectory using a central force gravity model and accelerometer measurements. Energy loss due to atmospheric drag acting on the spacecraft after separation is significant for steep entry cases

cases and must be accounted for in the release timing. An exponential atmospheric density model is carried on-board and refined by filtering accelerometer measurements using an EKF. The atmospheric density model is used to propagate the spacecraft trajectory to the atmospheric exit point to estimate energy loss after ballute separation. When the current orbital energy minus the predicted post-separation energy loss is less than the energy of the desired orbit, the ballute is released. The separation algorithm block diagram and flow chart are presented in figures 16 and 17.

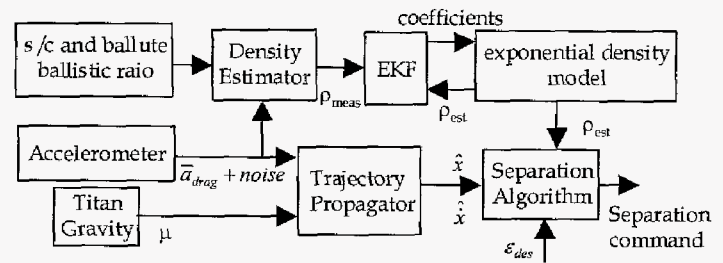


Figure 16. Separation algorithm block diagram

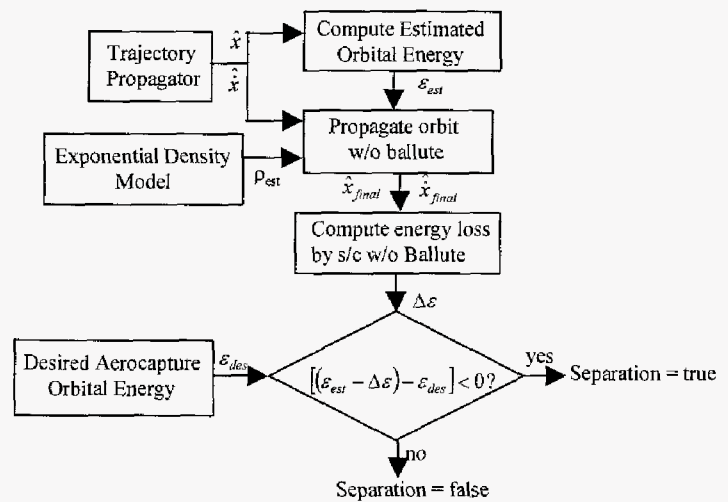


Figure 17. Separation algorithm flow chart

Separation algorithm performance was investigated for a Titan mission. Performance is evaluated in terms of the aerocapture success rate and the  $3\sigma$   $\Delta V$  required to circularize the orbit after aerocapture completion. The circularization  $\Delta V$  and success rate were determined from the results of a 2001 case Monte Carlo simulation. Atmospheric density uncertainty, trajectory delivery and knowledge errors, spacecraft and ballute drag coefficient uncertainties and accelerometer errors were randomized in the Monte Carlo simulation. Titan's atmospheric density was modeled using TitanGRAM, which includes random density perturbations superimposed on the mean density which can be varied over the  $3\sigma$  range by setting the Fminmax parameter from -1 to 1 with a value

of 0 representing the nominal atmosphere. The density variation with latitude at the expected arrival date was modeled using the following expression for Fminmax

$$F_{minmax} = 0.46 * \sin(lat) \cdot 0.54$$

Trajectory error analysis results<sup>2</sup> indicate an entry FPA delivery error of 0.9 degrees (3σ) and an entry FPA knowledge error of 0.3 degrees (3σ). Spacecraft and ballute ballistic coefficient errors of 5% (3σ) and accelerometer errors consistent with the Honeywell QA3000-30 specification were also used in the Monte Carlo simulation. The spacecraft and ballute physical properties are given in table 3. The 2001 case Monte Carlo results are shown in figures 18-21 and corresponding 3σ values are listed in table 4. It is clear from figures 4 and 5 that the mean apoapsis altitude is significantly higher than the target value of 1700 km especially for low periapsis altitude cases. This is a result of over-estimation of density by the on-board density model (EKF), which causes a slightly early ballute release to occur. Options for improving this aspect of the separation algorithm are under investigation.

Parameter	Value
Titan Entry Velocity	6.5 km/sec
Apoapsis of Aerocapture Orbit	1700 km
Ballute Frontal Area	750 m <sup>2</sup>
Spacecraft Frontal Area	3 m <sup>2</sup>
Spacecraft Mass	1000 kg
Ballute Mass	42 kg
Spacecraft Drag Coefficient	0.75 continuum 2.2 free molecular
Ballute Drag Coefficient	1.3 continuum 2.38 free molecular

Table 3. Input Parameters for Monte Carlo Run

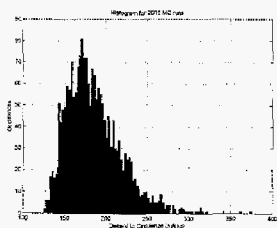


Fig 18 Circularization ΔV

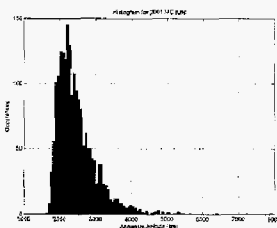


Fig 19 Apoapsis Altitude

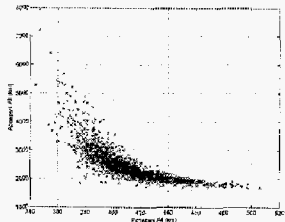


Fig 20 Apoapsis Vs Periapsis

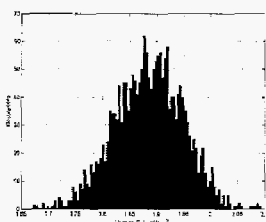


Fig 21 Peak Heating Rate

Parameter	Value
-----------	-------

Success Rate	100 %
Minimum Circularization ΔV	125 m/sec
Maximum Circularization ΔV	376 m/sec
Mean Circularization ΔV	186 m/sec
Mean + 3-sigma Circularization ΔV	285 m/sec
Mean Heating Rate	1.9 W/cm <sup>2</sup>
Mean + 3-sigma Heating Rate	2.1 W/cm <sup>2</sup>

Table 4. 2001 Case Monte Carlo Simulation Results

Mission	Range of Practical V(inf) (km/s)	Approximate Delta V (km/s)	Atm Density (kg/m <sup>3</sup> ) at Periapsis	Ballute Mass Savings for 500 kg On-Orbit
Mars				
Titan	6-10			
Neptune				
Venus				
Earth				

## Summary

System level analysis efforts conducted for NASA's Gossamer and In Space Propulsion programs illustrate the enormous performance benefits available for missions to planetary bodies with an atmosphere. Using ballutes for aerocapture results in an improvement of the effective specific impulse by more than a factor of three, when compared with typical bi-propellant chemical systems used for orbit insertion. Even as compared with structural aeroshells, design, operational and mass performance benefits are significant. More specifically, mass savings come from elimination of the aeroshell system. Additional savings are available by simplifying the spacecraft structure by removing many of the constraints placed upon it by the aeroshell architecture, such as thermal control system required to route heat out of the aeroshell. Additionally, ballutes are significantly less demanding on packaging and configuration for the system. While those for a Titan orbiter a mass savings of ~300 kg or 40% of the spacecraft dry mass is possible by using a ballute instead of a hard aeroshell to perform aerocapture.

Future efforts for advancing this technology will require definition of technology validation via an Earth flight test.

## Acknowledgments

Funding for this study was provided by the NASA Office of Space Science. The authors would like to thank Bonnie James and Michelle Munk at the MSFC In Space Propulsion Program office for their sponsorship and

guidance in the management of these efforts, as well as Jennifer Dooley at JPL, who managed the Gossamer study that was a basis for some of the cited efforts. The authors would like to thank Doug Gulick, Lockheed Martin Astronautics, George Sapna, ILC Dover, Peter Gnoffo, Langley Research Center, and Scott Inlow, Ball Aerospace & Technologies, Corp., who made significant and substantial contributions to the body of work used for development of this paper. Some of the work described was performed at the Jet Propulsion Laboratory (JPL), California Institute of Technology under contract with National Aeronautics and Space Administration (NASA).

### References

- <sup>1</sup> Hall, J., TBR.
- <sup>2</sup> Masciarelli, J., and Westhelle, C.,
- <sup>3</sup> Gnoffo, P. A., "An Upwind-Biased, Point-Implicit Relaxation Algorithm for Viscous, Compressible Perfect-Gas Flows," NASA TP-2953, Feb. 1990.
- <sup>4</sup> Gnoffo, P. A., "Computational Aerothermodynamics in Aeroassist Applications," AIAA 2001-2632, 15th AIAA Computational Fluid Dynamics Conference, Anaheim, CA, June 2001.
- <sup>5</sup> Bird, G. A., "Molecular Gas Dynamics and the Direct Simulation of Gas Flows," Clarendon Press, Oxford, 1994.
- <sup>6</sup> LeBeau, G. J., and Lumpkin II, F.E., "Application Highlights of the DSMC Analysis Code (DAC) Software for Simulating Rarefield Flows," Computer Methods in Applied Mechanics and Engineering, Vol. 191, Issue 6-7, 2001, pp. 595-609.